Toward development of feedback control system for wall turbulence with MEMS sensors and actuators

Takashi YOSHINO, Motoki TSUDA, Yuji SUZUKI, and Nobuhide KASAGI
Department of Mechanical Engineering, The University of Tokyo,
Hongo 7-3-1, Bunkyo-ku, Tokyo, 113-8656, Japan
yoshino@thtlab.t.u-tokyo.ac.jp

A prototype system for feedback control of wall turbulence control is developed, and its performance is evaluated in a physical experiment. Arrayed micro hot-film sensors with an 1mm spanwise spacing are employed for the measurement of streamwise shear stress fluctuations, and arrayed magnetic actuators having 3mm in diameter are used to introduce control input through wall deformation. The frequency response of the sensors and actuators is found to be sufficiently high for the flow condition presently considered. A digital signal processor was employed to drive output voltage for actuators, which is proportional to the instantaneous wall shear stress measured. It is found through the cross-correlation measurement between the wall shear stress and the wall deformation that the present control system has a time delay of 2.2 ms between sensing and actuation, which is smaller than the characteristic time scale of turbulence. The wall-normal fluctuations above the actuator is significantly increased at y^+=6, which indicates that the present actuators can introduce sufficiently large disturbances into the flow field.

1. Introduction

In the last decade, feedback control of wall turbulence attracts much attention because of its potential of high control performance with small energy input (e.g., Moin & Bewley, 1994; Gad-el-Hak, 1996; Kasagi, 1998). In such a control system, the near-wall coherent structures, which are responsible for the turbulent transport mechanism, should be detected by sensors mounted on the wall, and selectively manipulated by the motion of actuators. Although the spatio-temporal scales of the coherent structures are generally very small, recent development of microelectromechanical systems (MEMS) technology has made it possible to fabricate flow sensors and mechanical actuators of submillimeter scale (e.g., Ho & Tai, 1996).

Recently, Endo et al. (2000) carried out direct numerical simulation of turbulent channel flow, in which arrayed wall shear stress sensors and wall-deformation actuators of finite spatial dimensions are assumed. They developed a realizable control algorithm based on physical arguments on near-wall coherent structures, and found that drag reduction of 12% can be achieved by attenuating near-wall streamwise vortices. Morimoto et al. (2001) employ genetic algorithms to develop a simple feedback scheme based on the streamwise wall shear stress, and obtained drag reduction by using local wall blowing/suction. These findings encourage us to develop a feedback control system using distributed micro sensors and actuators in a laboratory experiment.

The objectives of the present study are to develop a prototype of feedback control system for wall turbulence with arrayed micro shear stress sensors and wall-deformation actuators, and to evaluate their performance in physical experiment in a wind tunnel.

2. Feedback control system of wall turbulence

Figure 1 shows a schematic diagram of feedback control system for wall turbulence. Several rows of arrayed micro sensors aligned in the spanwise direction are mounted flush on the wall, and staggered arrays of actuators are placed in between. In the present study, hot-film sensors are employed for the measurement of the streamwise wall shear stress, while magnetic actuators are used to introduce control input into the flow field by wall-deformation. In the present study, a single row of 8 hot-film sensors with a spanwise spacing of 1mm are used as shown in Fig. 2. Two rows of arrayed actuators with a 4 mm spacing are arranged with a 2 mm offset in the spanwise direction, and consequently five actuators are located with a 2 mm spanwise

spacing. These spanwise spacings of the sensors and actuators are respectively about 10 and 20 wall units under the flow condition described later. A digital signal processor (DSP) board (SMT-326, Sundance DSP Inc.) with 32 channel analog inputs and analog outputs is used as the controller of the present system. The output voltage of the constant temperature circuits for hot-film sensors are firstly digitized with 16 bit AD converters. The control signals for the actuators are then computed with a DSP (C44, 60MFLOPS) and converted back to analog signals using 16 bit DA converters. The present DSP system has an inherent time delay of 1.6 ms due to the data transfer and processing inside.

3. Micro wall shear stress sensor

Figure 3 shows a schematic of the micro shear stress sensor used in the present study. A platinum thin-film heater is deposited on a Si_3N_4 diaphragm of 1 μm in thickness. In order to keep a sufficiently large electric resistance of the heater, the thin line of platinum is patterned zigzag in an area of 200×23 μm^2. An air cavity of 200 μm in depth is formed underneath the diaphragm for reducing thermal loss to the substrate. Another platinum resistor is made on the substrate and used for temperature compensation. The length of the heater is 200 μm and the dimensions of the diaphragm is 400×400 μm^2.

Figure 4 shows the root-mean-square value of the streamwise wall shear stresses $\tau_{u\,rms}$ normalized by its mean value $\tau_{u\,mean}$. It is found in DNS studies (e.g., Moser et al., 1999; Iwamoto et al., 2001) that $\tau_{u\,rms}/\tau_{u\,mean}$ is weakly dependent on the Reynolds number and equal to about 0.36-0.4. It is shown by the present experiment in a turbulent air channel flow that the measurement data using the present shear stress sensors is decreased with increasing Reynolds number due to their imperfect frequency response, but the data are in accordance with the DNS result at $Re\tau<400$.

The spanwise two-point correlation of τ_u obtained with the arrayed sensors is shown in Fig. 5. The present data exhibit a negative peak at $\Delta z^+ \sim 50$, and are in good accordance with the DNS data. Therefore, the near-wall coherent structures, which are the target of the feedback control, can be well captured with the present wall shear stress sensors.

4. Wall-deformation magnetic actuator

Figure 6 shows a schematic of wall-deformation magnetic actuator. Silicone rubber having 0.1 mm in thickness is used as a elastic membrane, and a rare-earth miniature permanent magnet of 1 mm in diameter is glued on the backside. A miniature copper coil (500 turns), of which outer diameter is 3 mm, is placed underneath the magnet. Figure 7 shows a static response of the actuator. The displacement is a nonlinear function of the voltage applied, and about 100 μm deformation is obtained with 4 V voltage. Figure 8 shows the dynamic response of the actuator as a function of frequency of the sinusoidal driving voltage. Because the spring constant of the membrane is increased with increasing the deformation as shown in Fig. 7, the resonant frequency depends on the voltage amplitude; the resonant frequency is increased from 450Hz to 600Hz for 1-4 $V_{p\text{-}p}$ signal. The time constant required for the experimental condition described later is about 7ms, so that the frequency response of the actuator should be sufficiently high.

The effect of the wall-deformation actuator on the surrounding fluid is examined in a quiescent air chamber (160×160×160 mm^3). Figure 9(a) shows the flow visualization near the actuator driven with 400Hz sinusoidal signal. The maximum deformation is 200μm. It is shown that when the actuator reaches its maximum height, its shape looks like a frustum, and the flow around the actuator is spread out from the center. The flow around the actuator was also measured with 2-component laser Doppler velocimetry (Dantec Dynamics Inc., 60X61). The phase-averaged velocity vectors are shown in Fig. 10(b). The maximum fluid velocity obtained at the elevation twice the maximum displacement of the actuator is about 0.25 m/s, which is about half of the maximum wall-deformation velocity.

5. Evaluation of prototype control system

The present prototype system is evaluated in a turbulent air channel flow. The channel width and height are 50 and 500 mm, respectively. The test section is located 80*H* downstream from the inlet, where the flow is fully-developed. The bottom wall is equipped with the control system described above. The bulk mean velocity U_m is varied from 2.5 to 9.3 m/s, which corresponds to the Reynolds number Re_τ based on the wall friction velocity u_τ and the channel half-width from 250 to 800. When Re_τ=300 (U_m=3.0 m/s), one wall unit and viscous time unit respectively correspond to 0.09 mm and 0.5 ms. At this flow condition, the mean diameter of the near-wall streamwise vortices is estimated to be 2.7 mm, while its characteristic time scale is 5 ms.

The dynamic response of the control system is evaluated by using a simple feedback scheme, in which the actuator driving signal is set to be proportional to the instantaneous wall shear stress fluctuation. The deformation of the actuator is measured with a laser displacement meter, while the DSP continuously update the driving voltage of the actuator. Figure 10 shows the cross correlation of the shear stress fluctuation and the displacement of the actuator. The correlation peak appears at 2.2 ms, which indicates that the present control system has a time delay of 2.2 ms between the sensor input and the actuator displacement. Since the characteristic time scale of the streamwise vortices is 5ms, the present control system should have a potential to manipulate the vortices effectively. It is noted that most of the time delay is caused by the DSP itself. Faster controller using field programmable gate array (FPGA) having 256 channel analog input/output is now developing. By using the FPGA, the inherent time delay of the controller is decreased to less than 0.2 ms, thus the total time delay should be decreased to 0.8 ms.

Figure 11 shows the experimental setup for the LDV measurement above the actuator. In order to measure the streamwise and wall-normal velocity fluctuations near the wall, two-component LDV system using three laser beams is employed, where one of the beam contains two color. The diameter of the beam is 1.35 mm and the focal length of the lens is 400 mm. The measurement volume is about 190×190×5500 μm^2. Smoke particles of about 1μm diameter, which are generated by the SAFEX® fog generator (Dantec Dynamics Inc., FOG 2010) are used as flow tracers. Figure 12(a) shows the streamwise mean velocity profiles. Mean velocities both for unmanipulated and manipulated flows are in good agreement with the DNS result. Figure 12(b) shows the rms values of the velocity fluctuations. Although the streamwise component is unaffected by the motion of actuator, the wall-normal velocity fluctuations are significantly increased at y^+=6. Since the magnitude of v_{rms} is much larger than that employed in previous DNS studies for active control of wall turbulence, the present actuators should introduce sufficiently large control input into the flow field.

Figure 13 shows a prototype of magnetic MEMS actuator recently developed. The dimension of the flap is about 1mm×2mm, which is much smaller than the actuator shown in Fig. 6. The flap made of polyimide is suspended with a pair of hinges in the middle of the flap. By using this seesaw configuration, we can obtain large displacement as well as high frequency response. Permanent polymer magnet is formed on the backside of the flap, and the flap is driven by the magnetic force between the polymer magnet and miniature coil underneath. At this moment, the displacement of the prototype is 10 μm, but it should be improved by tuning the fabrication process.

6. Conclusion

The prototype of the feedback control system for wall turbulence is developed with arrayed micro hot-film sensors and arrayed wall-deformation magnetic actuators. The dynamic response of the sensors and actuators are found to be sufficiently high for the experimental condition employed. The time delay of the feedback loop of the present control system was estimated to be 2.2 ms, where the time delay in the DSP is the major cause. It is found in the LDV measurement that the present control system can introduce sufficiently large control input to the flow field.

The authors are grateful to Mr. S. Kamiunten in Yamatake Corp. for his corporation in manufacturing micro shear stress sensors.

Reference

Endo, T., Kasagi, N., and Suzuki, Y., 2000, Int. J. Heat Fluid Flow, 21, 568.

Gad-el-hak, M., 1996, Appl. Mech. Rev., 49, 377.

Ho, C.-M., and Tai, Y.-C., 1996, ASME J. Fluids Eng. 118, 437.

Iwamoto, K., Suzuki, Y., and Kasagi, N., 2001, 2nd Int. Symp. Turbulence and Shear Flow Phenomena, Stockholm, vol. III, 17.

Jiang, F., Tai, Y.-C., Gupta, B., Goodman, R., Tung, S., Huang, J.-B., and Ho, C.-M., 1996, Proc. IEEE Workshop on MEMS, 110.

Kasagi, N., 1998, Int. J. Heat & Fluid Flow, 19, 134.

Moin, P., and Bewley, T., 1994, Appl. Mech. Rev., 47, S3.

Morimoto, S., Iwamoto, K., Suzuki, Y., and Kasagi, N., 2001, Bull. Am. Phys. Soc., 46, 185.

Moser, R. D., Kim, J., and Mansour, N. N., 1999, Phys. Fluids, 11, 943.

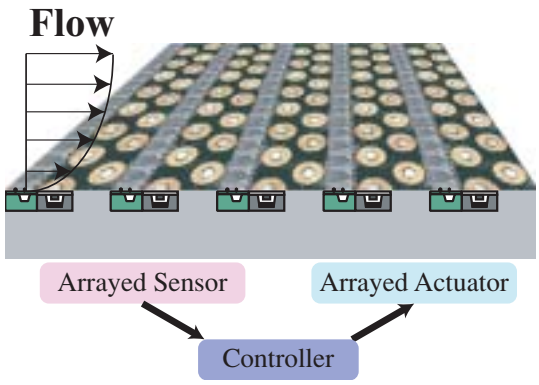

Fig. 1 Schematic diagram of active feedback control system for wall turbulence.

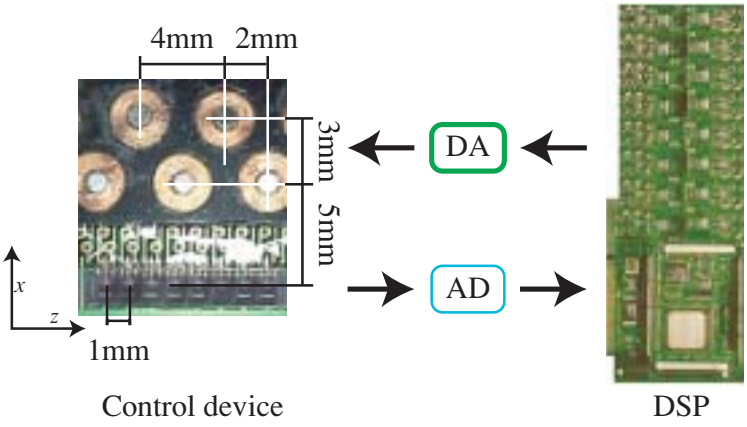

Fig. 2 Prototype system for wall turbulence control with arrayed sensors and actuators.

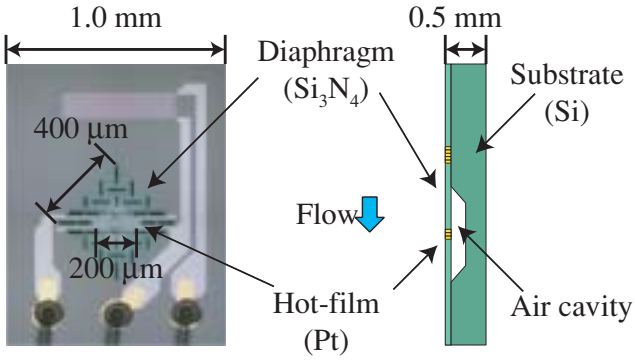

Fig. 3 Magnified view of micro hot-film shear stress sensor.

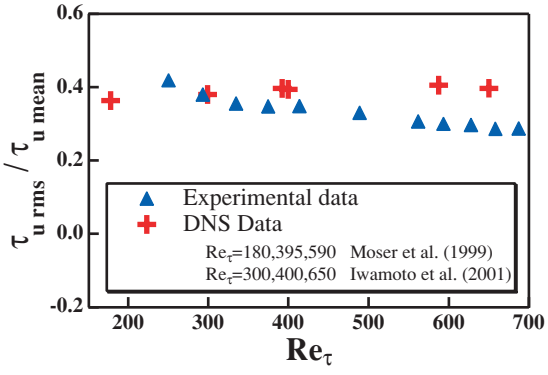

Fig. 4 Rms values of wall shear stress fluctuations.

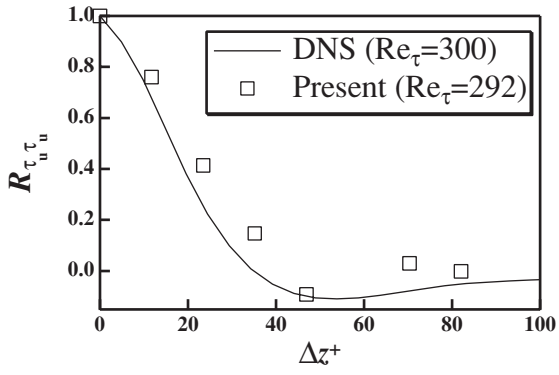

Fig. 5 Spanwise two-point correlations of the streamwise shear stress fluctuation.

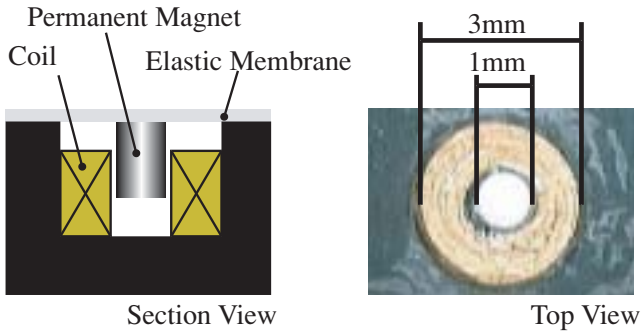

Fig. 6 Schematic of wall-deformation magnetic actuator.

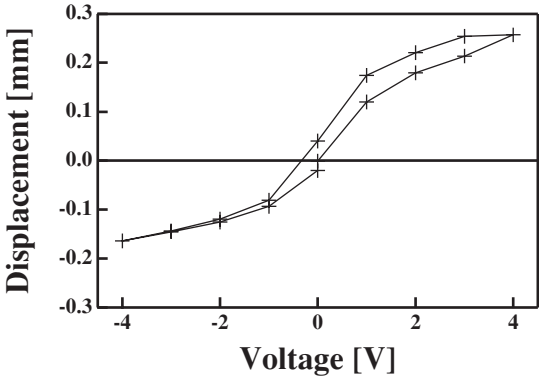

Fig. 7 Static response of wall-deformation magnetic actuator.

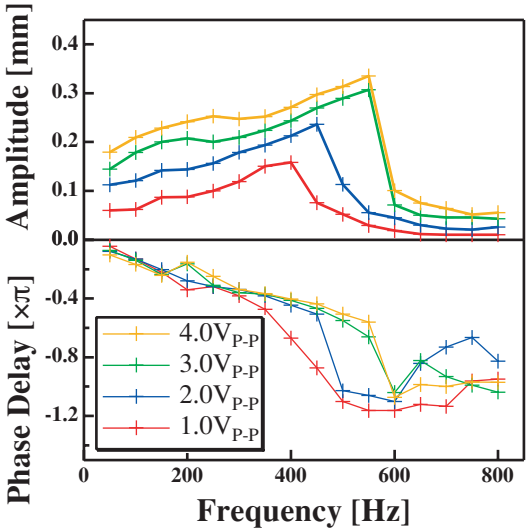

Fig. 8 Dynamic response of wall-deformation magnetic actuator.

a)

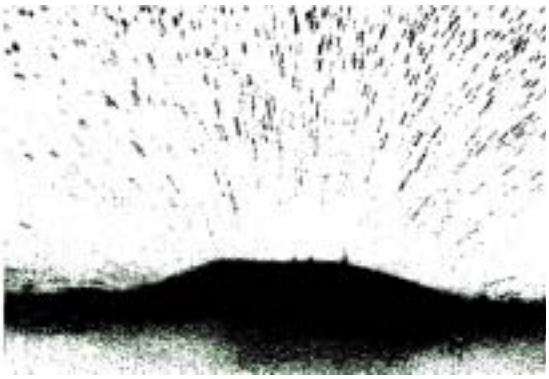

b)

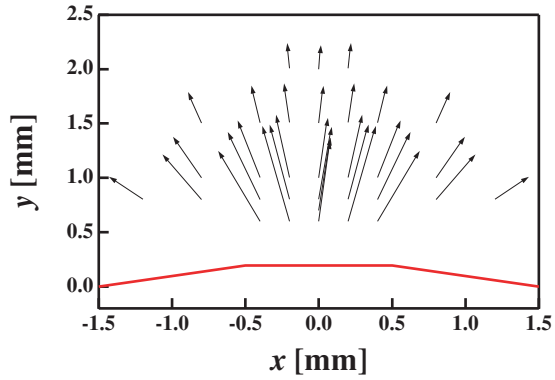

Fig. 9 Velocity field around wall-deformation actuator. a) Flow visualization, b) LDV measurement.

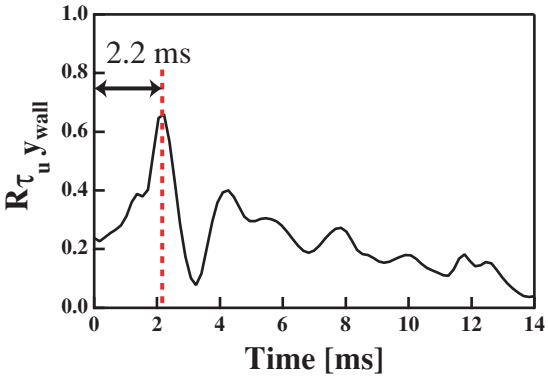

Fig. 10 Cross correlation of the streamwise shear stress fluctuation and actuator displacement.

a) b)

Fig. 11 LDV measurement setup. a) 2-component LDV probe and its traversing system, b)Top view of the control system and 3 laser beams crossing above a magnetic actuator.

a) b)

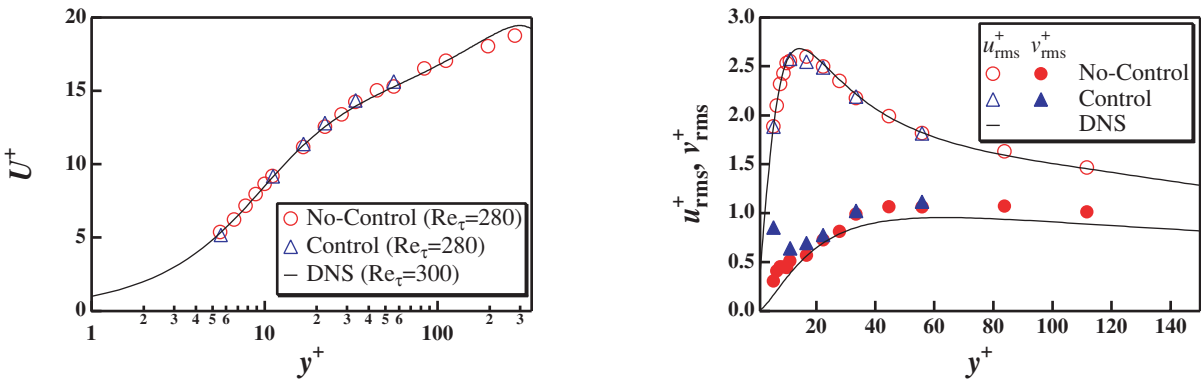

Fig. 12 Velocity measurement above the actuator in turbulent channel flow.
a) Streamwise mean velocity, b) Streamwise and wall-normal velocity fluctuations.

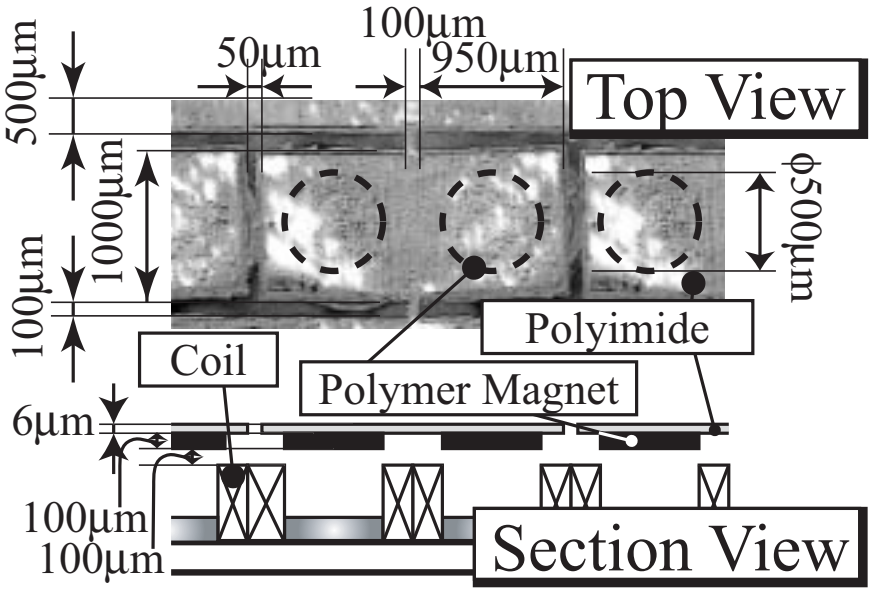

Fig. 13 Prototype of MEMS magnetic actuators.